MAE 598 Design Optimization

Performance Optimization of the Suspension System of an Off-Road Vehicle

A Project Report By

Aniket Borude
Gaurav Kankriya
Suhailjeet Singh
Vrushali Manka

Spring 2016
Arizona State University
School for Engineering of Matter, Transport, and Energy

Abstract

Suspension system of a vehicle is the system of tires, tire air, springs and linkages that connects a vehicle to its wheels and allows relative motion between the two. Suspension systems control handling of the vehicle, comfort of the occupants and ride quality by isolating the vehicle from road noise, bumps, vibrations, etc. A vehicle needs to maintain a balance of all these goals, so the design of suspensions involves finding the right compromise.

Project deals with the performance optimization of a suspension system of an off-road vehicle. Scope of this project is to deal with the performance parameters, controllability, durability, comfort and rolling resistance performance of tire. The overall system is divided into four individual subsystems which have their own objective functions and constraints and are optimized individually.

The four subsystems considered are:

1. Optimization of vertical acceleration of sprung mass
2. Optimization of geometric parameters of the wishbone suspension system for vehicle performance improvement
3. Minimization of the deformation to effectively reduce the tire rolling resistance
4. Optimization of strain energy in the tire to improve the durability potential by varying the steel belt angles

Acknowledgement

Nomenclature and Symbols

A	Road irregularity coefficient ($m^2/(\frac{rad}{m})$)
B	Bound of mean square value of jerk (m/s^3)
K	Suspension Stiffness (N/m)
K_t	Tire Stiffness (N/m)
C	Damping force coefficient (N/m/s)
f_d	Suspension travel clearance (m)
f_s	Suspension static deflection (m)
G	Tire ground Static Load (m)
V	Vehicle speed (m/s)
g	acceleration due to gravity (m/s^2)
m_1	unsprung mass (Kg)
m_2	sprung mass (Kg)
P	Tire ground dynamic load (Kg)
S(Ω)	power spectral density of Road Profile (m^3)
η	coefficient for bumping
ξ	coefficient of acceleration
Ω	Spatial Frequency (rad/m)
z	vertical displacement of sprung mass (m)
$\overline{\ddot{z}^2}$	mean square value of vertical acceleration of vehicle body $\left(\frac{m}{s^2}\right)^2$
$\overline{\dddot{z}^2}$	mean square value of vertical jerk of vehicle body $\left(\frac{m}{s^3}\right)^2$
$\overline{(P/G)}$	mean square value of relative tire-ground dynamic load
ל	vertical displacement of un-sprung mass (m)
q	elevation of road surface (m)
a	length of DW (Double wishbone suspension) link MA (mm)
b	length of DW suspension link AB (mm)
c	length of DW suspension link BN (mm)
d	length of DW suspension link MN (mm)
θ_0	orientation of link MN with respect to vertical (°)
θ_2	orientation of link MA with respect to link MN (°)
θ_3	orientation of link AB with respect to link MN (°)
θ_4	orientation of link BN with respect to link MN (°)
θ_{30}	initial angle that arm AB makes with MN when the DW suspension system is in a dynamic state of balance (°)
A_x	x-coordinate of point A in DW suspension system (mm)
A_y	y-coordinate of point A in DW suspension system (mm)
B_x	x-coordinate of point B in DW suspension system (mm)
B_y	y-coordinate of point B in DW suspension system (mm)

Table of Contents

1. Subsystem 1: Optimization of Vertical acceleration of sprung mass (Suhail Jeet Singh)

1.1 Problem Statement

The primary purpose of a suspension system of a vehicle is to ensure excellent ride comfort and good handling at all times, irrespective of the road irregularity. The road irregularity may be due to different sources such as potholes, bumps and non-uniformity of the tire/wheel assembly which acts as the major source of vibration of the sprung mass through the tire/wheel assembly and the suspension system. This is also important for the durability of the parts since increased vibrations wares out the parts of the suspension system.

In this report we are going to concentrate mainly on reducing the vertical acceleration of a passive suspension system (which will be our objective function) with the dynamic tire load, rattle space and jerk as the constraints for the system.

1.2 Assumptions made

1. The road profile is considered the same on both the sides of the vehicle which follows the Gaussian distribution given by

    $S(\Omega) = \frac{A}{\Omega^2}$

    Where the value of A (road irregularity coefficient) depends on the profile of the road

    Table1.1 Vehicle speeds and coefficient of road irregularities

	Vehicle speed (m/s)	A (m^3)
Case 1	40	6.5×10^{-6}
Case 2	30	12×10^{-6}
Case 3	20	20×10^{-6}

2. The tire never leaves the ground
3. Vehicle mass distribution coefficient is considered as constant
4. The tire mass is lumped mass and the tire distributed stiffness to be concentrated stiffness and the tire damping is neglected

Suspension damping is assumed to be viscous damping. The contact between suspension and the bumper is neglected since it is assumed that the distance between them is very large and the probability of contact is very small.

1.3 Modeling

Figure 1 shows a simplified version of a passive suspension system of a quarter car model. Consists of a sprung mass m_1, un-sprung m_2, suspension damping C, spring stiffness K, Tire stiffness K_t. We are going to develop the model in the form of a Non-linear programming problem which will be used in our optimization study

The nominal values of the quarter car model for an off road vehicle are m_1=98 Kg, m_2=803 Kg, K_t=204394 N/m, K=63528 N/m, C=3428 (N/m/s)

$$m_2\ddot{z}+C(\dot{z}-\dot{ל})+K(z-ל)=0 \qquad \ldots (1)$$
$$m_1\ddot{ל}+m_2\ddot{z}+K_t(ל-q)=0 \qquad \ldots(2)$$
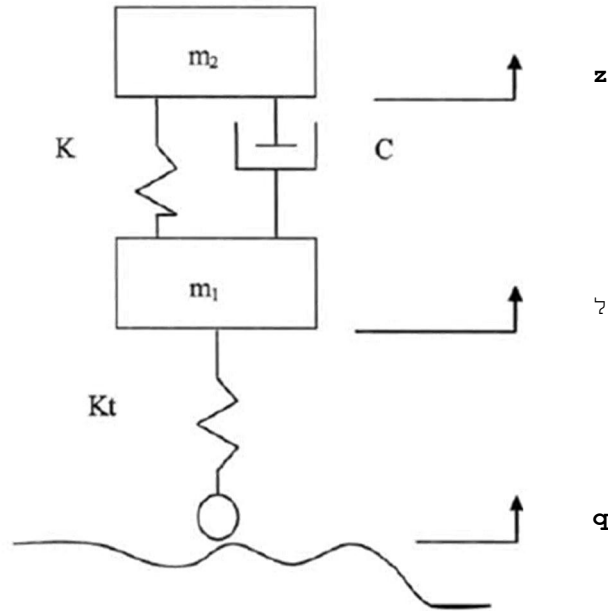
Figure 1: Vehicle suspension model of a 2 DOF passive suspension

Here we are going to describe the ride performance by the root mean square value of the vertical acceleration of the vehicle body by $\bar{\ddot{z}}$. This will be our primary design criterion and the objective function to be minimized.

i.e. minimize vertical body acceleration $\bar{\ddot{z}}$

Performing Laplace transform on equations 1 and 2 we can evaluate the transfer function $\frac{\bar{\ddot{z}}}{q}$ and from there we get the following equation for the mean square value of vertical acceleration.

$$\bar{\ddot{z}}^2 =\left(\frac{\pi AV}{m_2^2}\right)\left[K_tC + \frac{(m_1+m_2)K^2}{C}\right] \quad \text{Objective function}$$

Constraints:

1. **Relative dynamic Load**:- We have made an assumption that the tire must never leave the ground but in fact some probability is represented in the time domain by the value of b_o. This means that the road holding capability must not be above a certain value. Analytically this means.

$$g_{1=} \overline{(P/G)}^2 \times b_o^{-1} - 1 \leq 0$$

Where $\overline{(P/G)}^2 = \left(\frac{\pi A V}{g^2}\right)\left(\frac{m_1}{C}\right)\left[\left[\frac{K_t}{(m_1+m_2)} - \frac{K}{m_2}\right]^2 + \frac{K^2}{m_1 m_2} + \left(\frac{C}{m_2}\right)^2 \frac{K_t}{m_1}\right]$

2. **Rattlespace**: - Since we have made the assumption that the bumper hitting in quarter quarter car model is very less, there is a need to limit the suspension travel in order to avoid that from happening. An empirical design to avoid this from happening is given by

$f_d = 3 f_s^{0.5}$
This leads to

$$g_{2=} \left(\frac{\eta}{3\xi}\right)\left(\frac{m_2 g}{2}\right)^{0.5}\left[\frac{C^2 K_t}{K(m_1 + m_2)} + K\right]^{-0.5} - 1 \leq 0$$

The value of η and ξ are associated with bumper hitting and cargo throwing which can be selected as η=3 and ξ=2 for off road vehicles.

3. **Jerk:** - In the recent study it has been suggested that jerk also plays a vital role in determining the comfort level of the passenger and for that very purpose we have included it as the third constraint. For passenger comfort according to ISO 2631 standards jerk should not be more than $18 \frac{m}{s^3}$

$$g_{3=} \left(\frac{\pi A V}{m_2^2}\right)\left[\frac{K_t^2 C}{m_1} + \frac{K_t K^2}{C}\right] - B \leq 0$$

We can include additional constraints to our objective function but in this report we will concentrate on the major constraints given above. As mentioned earlier we will try and minimize the acceleration of the sprung mass with the above given design constraints. The design variables are chosen as $m_1,\ m_2,\ K_t, K, C$ and the design parameters are chosen as A and V

$$\text{Minimize } \overline{\ddot{z}}^2 = \left(\frac{\pi A V}{m_2^2}\right)\left[K_t C + \frac{(m_1+m_2)K^2}{C}\right]$$

4

Subjected to constraints below

$$\left(\frac{\pi AV}{g^2}\right)\left(\frac{m_1}{C}\right)\left[\left[\frac{K_t}{(m_1+m_2)}-\frac{K}{m_2}\right]^2+\frac{K^2}{m_1 m_2}+\left(\frac{C}{m_2}\right)^2\frac{K_t}{m_1}\right]\leq b_o$$

$$\left(\frac{\eta}{3\xi}\right)\left(\frac{m_2 g}{2}\right)^{0.5}\left[\frac{C^2 K_t}{K(m_1+m_2)}+K\right]^{-0.5}\leq 1$$

$$\left(\frac{\pi AV}{m_2^2}\right)\left[\frac{K_t^2 C}{m_1}+\frac{K_t K^2}{C}\right]\leq B$$

$$78.4\leq m_1\leq 117.6$$

$$642.4\leq m_2\leq 963.6$$

$$163515.2\leq K_t\leq 245272.8$$

$$50822.4\leq K\leq 76233.6$$

$$2742.4\leq C\leq 4113.6$$

In equation 3 the values of b_o is chosen as 0.27 and the value of B is taken as $18\frac{m}{s^3}$

1.4 Optimization Study

The optimization study is done in Matlab using SQP algorithm through fmincon. The initial guess points i.e. x_o is taken as

m_1=98 Kg, m_2=803 Kg, K_t=204394 N/m, K=63528 N/m, C=3428 (N/m/s)., V=40(m/s) A=6.5× 10^{-6} $(m^2/(\frac{rad}{m}))$, B= $18\frac{m}{s^3}$, b_o= 0.27

x0= [98; 803; 204394; 63528; 3428];

Table1.2. Optimum values obtained through SQP

	m_1	m_2	K_t	K	C
Optimum Values × 10^5	0.0011	0.0096	1.6352	0.5082	0.0274

Optimum value of acceleration = 1.2903 $\frac{m}{s^2}$

The above answers obtained are the optimum solution for our design variables with the given set of constraints and bounds. The below figures show the relationship of the sprung mass acceleration with the 5 design variables.
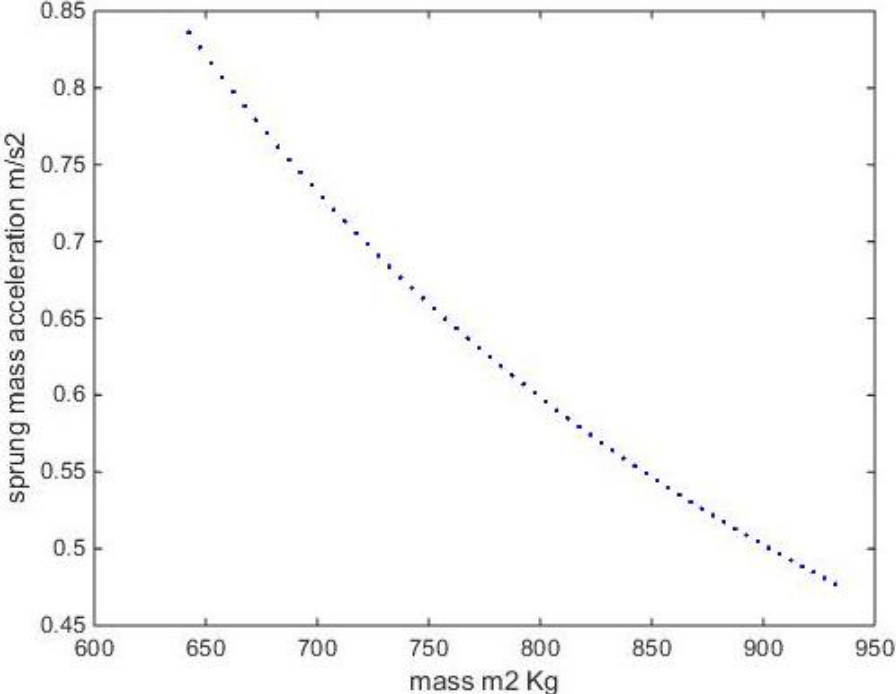

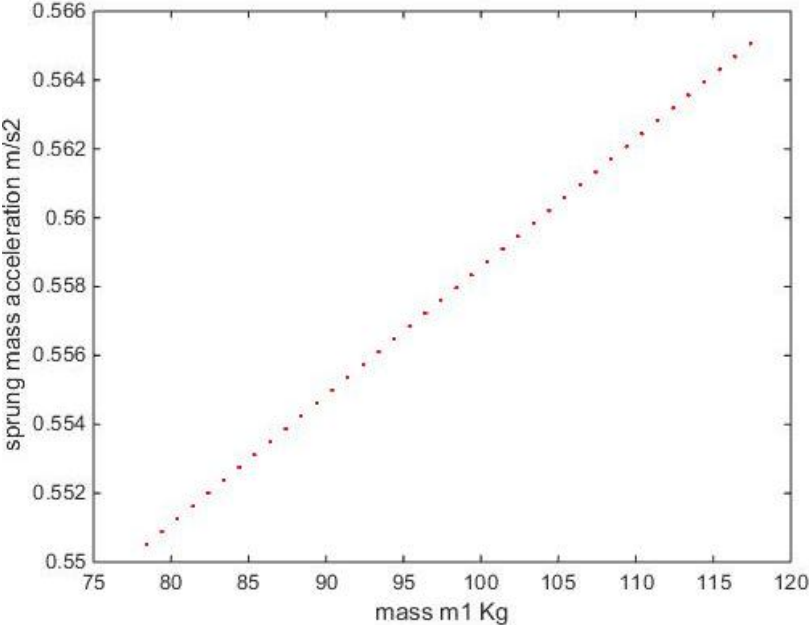Figure 1.2 : Sprung mass acceleration vs m_2

Figure 1.3: Sprung mass acceleration vs m_1
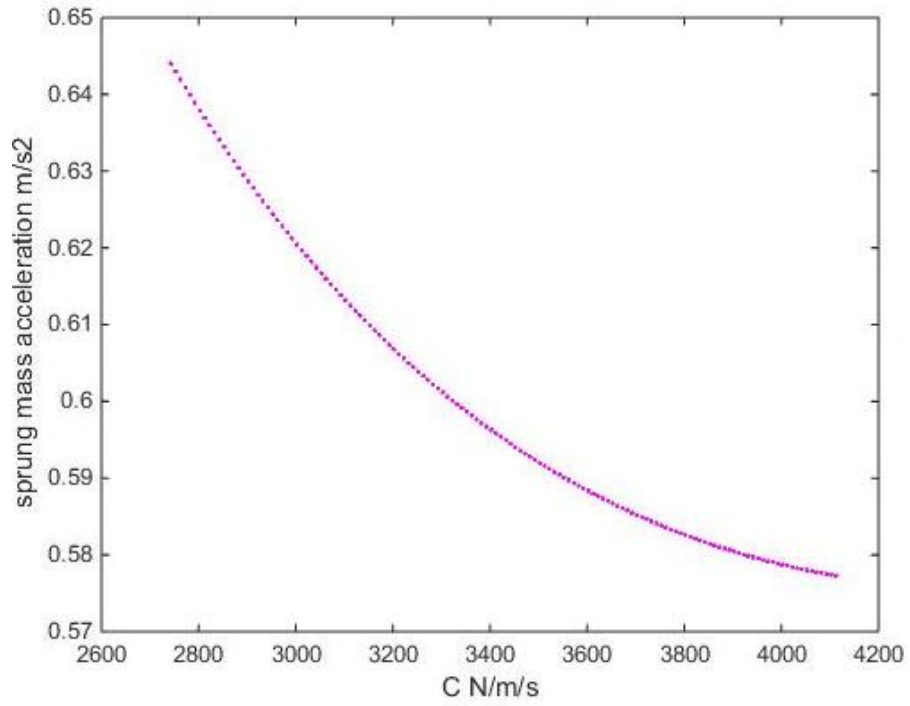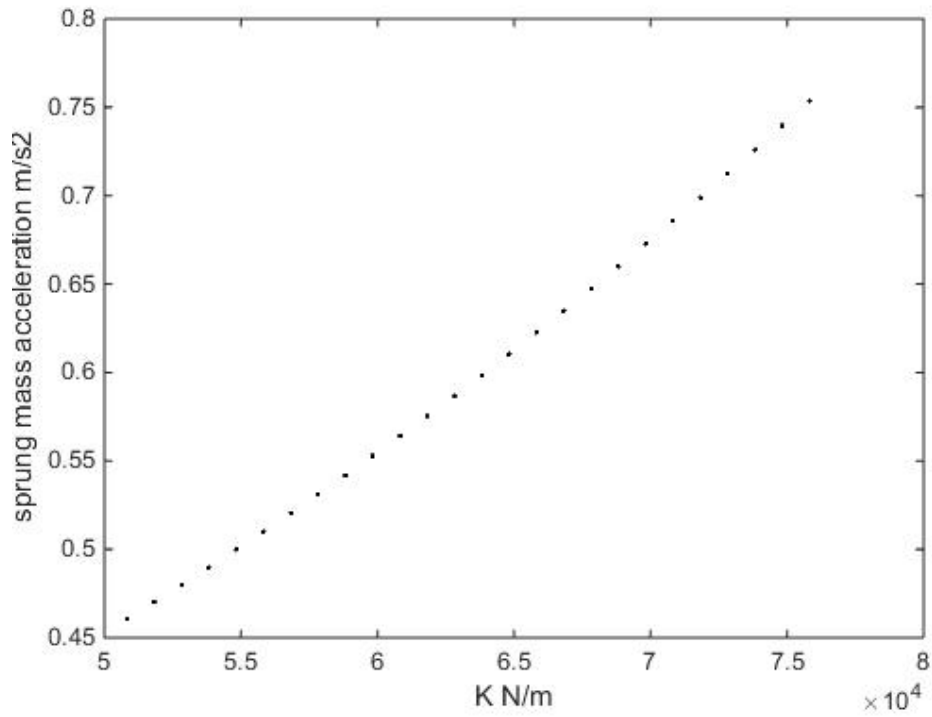
Figure 1.4: Sprung mass acceleration vs C

Figure 1.5: Sprung mass acceleration vs K
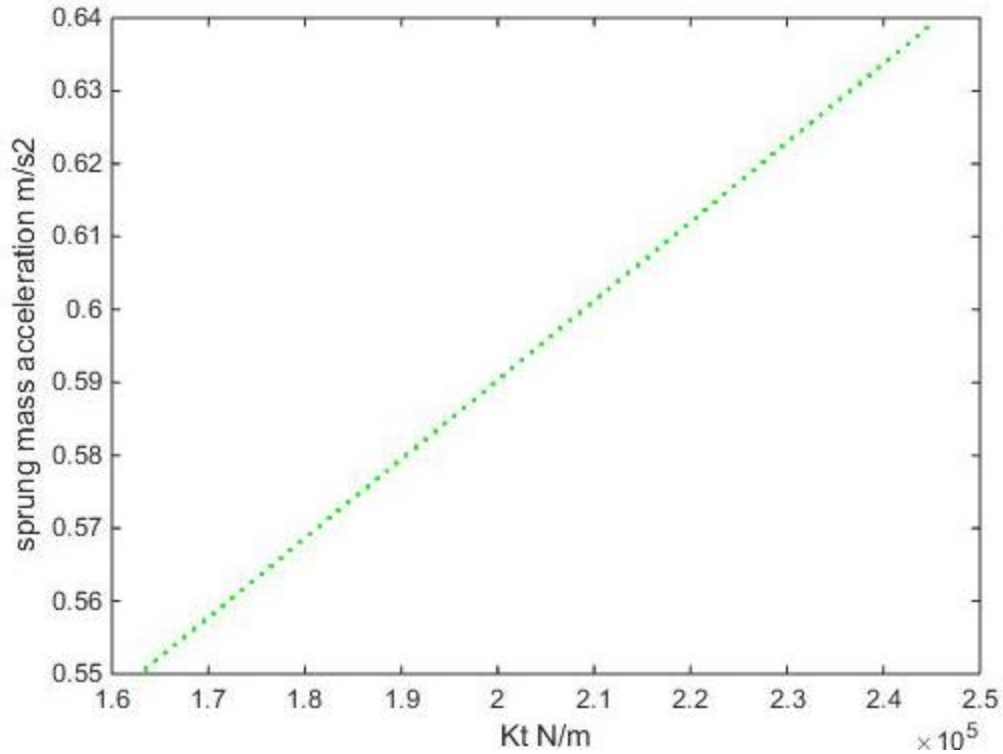
Figure 1.6: Sprung mass acceleration vs K_t

It can be seen from the graph that there is only one global optimum point as all design variables are either strictly increasing or decreasing with respect to the sprung mass.

By calculating the corresponding natural frequencies of the sprung and unsprung mass it was found that the sprung mass natural frequency was reduced to 0.366 Hz from the baseline frequency of 1.41 Hz and the unsprung mass natural frequency reduced to 5.94 Hz from 7.3Hz.It can also been seen that the Spring stiffness and the tire stiffness have also reduced from its baseline frequency. These results show that the optimum results obtained indeed increase the ride quality

1.5 Parameter Study

In this section we will be analyzing the effects of changing the important parameters of the design and we will see how these change in parameters effect the objective function and if we can deduce any relationship between them.

Table1.3 Change in Sprung acc by changing system parameters

Parameter to change		Value	Sprung Mass Acceleration $\frac{m}{s^2}$
Road irregularity coefficient	$A(m^2/(\frac{rad}{m}))$	6.5×10^{-6}	1.2903
		12×10^{-6}	2.23821
		20×10^{-6}	3.9701
Jerk	$B\frac{m}{s^3}$	18	1.2903
		24	1.1050
		50	1.0060
Velocity	$V\frac{m}{s^2}$	40	1.2903
		30	0.9677
		20	0.6451

It can be seen from the above table that with the increase in the value of road irregularity coefficient and velocity the RMS acceleration increases. Similarly with the increase in jerk there is a very slight increase in the RMS acceleration.

1.6 Conclusion

It can be seen that the results obtained by using the SQP algorithm through fmincon in Matlab optimizes the sprung mass, un sprung mass, spring stiffness, tire stiffness and suspension damping coefficient for given set of constraints given by Rattle space, Dynamic tire load and Jerk. The values obtained lie within the bounds specified at the beginning. We have also seen how different important design parameters such as Jerk, Velocity and road irregularity coefficient effect the RMS acceleration of the sprung mass.

2. Subsystem 2: Optimization of geometric parameters of the wishbone suspension system for vehicle performance improvement (Vrushali Manka)

2.1 Problem Statement

We are considering the suspension system of an off-road vehicle. During the motion of a vehicle, it encounters irregularities on the road, which can damage the components of the vehicle. To avoid this, vehicles have suspension systems. Suspension provides ride comfort to the driver and handling stability to the vehicle. Geometric parameters of the suspension system affect the camber greatly, which in turn affects the ride and handling characteristics by allowing the tires of the vehicle to maintain sufficient contact with the road. Here we are going to use the same concept and optimize the camber angle to improve the performance of the vehicle.

There are different kinds of suspension systems like MacPherson, Wishbone and Double Wishbone suspension system. We are considering the double wishbone suspension system for this off-road vehicle.
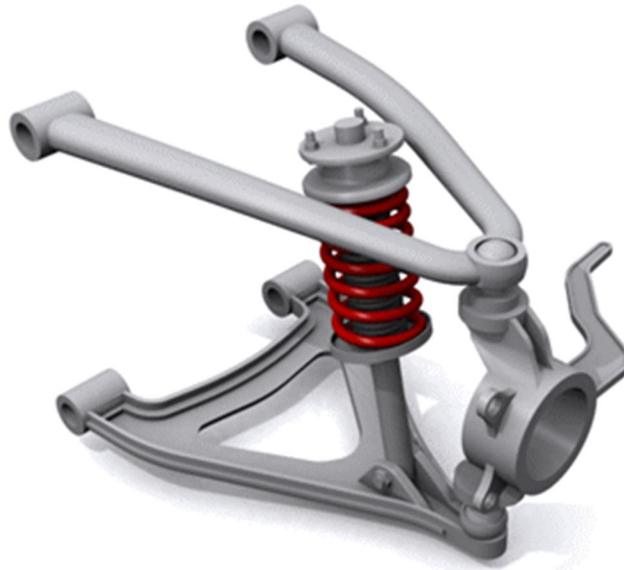

Fig. 2.1 Double Wishbone System [19]

The Fig. 2.1 depicts the double wishbone system, which looks like two A-arms connected at ends. It is also called an A-arm suspension system. There are many advantages of the DW suspension design. The lengths of upper and lower arms of this system are unequal. Due to this, the vertical suspension movement results in an increase in negative camber. So, during the turn, the outer tires do not lose contact with the road. In this system, the camber changes as the car rolls or takes a turn. In other systems, initial negative camber has to be provided, due to which the tires will be in negative camber even when the vehicle is moving straight. This causes the tires to wear. Thus, we are optimizing the double wishbone suspension system in this subsystem.

2.2 Modeling

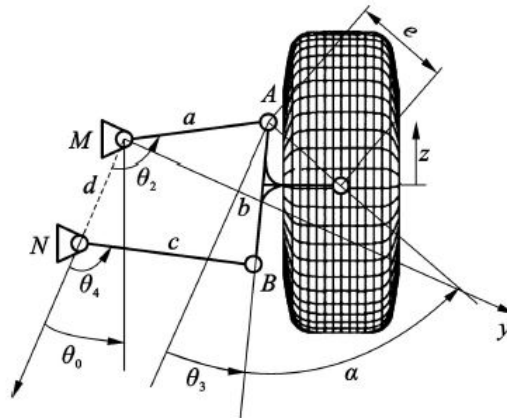The Fig. 2 shows the schematic diagram of this suspension system.

Fig. 2.2 Schematic diagram of DW suspension system

2.2.1 Objective of the optimization problem

Camber angle here is $\theta_3 - \theta_{30}$

Lengths and orientations of the links of the suspension system are the variables of the optimization problem. To formulate the objective of this problem, relation between the camber angle and other geometric parameters had to be determined. The calculations performed are as follows,

Point M in the figure is considered as the origin for the system, and Cartesian coordinates of all other points are determined according to this. So,

$$Mx = 0$$
$$My = 0$$
$$A_x = a\cos\,(\theta_2 - \theta_0 - 90)$$
$$A_y = a\sin\,(\theta_2 - \theta_0 - 90)$$
$$N_x = -d\sin(\theta_0)$$
$$N_y = -d\cos(\theta_0)$$
$$B_x = c\cos\,(\theta_4 - \theta_0 - 90) - d\sin\theta_0$$
$$B_y = c\sin\,(\theta_4 - \theta_0 - 90) - d\cos\theta_0$$
$$\tan\,(\theta_0 - \theta_3) = \frac{A_x - B_x}{A_y - B_y}$$
$$\boldsymbol{\theta_3 = \theta_0 - tan^{-1}(\frac{A_x - B_x}{A_y - B_y})}$$

This equation provides the variation in camber angle. Objective is to minimize the value of θ_3. So the above equation is the objective of this subsystem.

2.2.2 Constraints

The double wishbone system is actually a four bar linkage. And here the system is triple rocker, so this is a Non-Grashof four bar linkage. This gives us the following relation,

$$\mathbf{b + c \geq a + d}$$
$$\mathbf{a\cos(\theta_2) + b\cos(\theta_3) - c\cos(\theta_4) - d = 0}$$
$$\mathbf{a\sin(\theta_2) + b\sin(\theta_3) - c\sin(\theta_4) - d = 0}$$

For a double wishbone suspension system, considering the more efficient system called short-long arm suspension, it can be said that,

$a \leq c$

From the geometry as shown in the Fig. 2, the following relation is obtained,

$$\mathbf{a\sin(\theta_2 - 9\ 0 - \theta_0) - [c\sin(\theta_4 - 9\ 0 - \theta_0)] = b\cos(\theta_0 - \theta_3) - d\cos\theta_0}$$

θ_3 is included in this constraint equation, as can be seen from the above equation. So, while solving the optimization problem, we have to solve the simultaneous equations, objective and

11

this constraint for finding the values of both θ_4 and θ_3. This is calculated with the help of MATLAB function fsolve.

From force equilibrium,

$$F_s = Kdx$$

Y-component of Fs,

$$F_{sy} = 0.5Kc\sin(\theta_4 - 90 - \theta_0)$$

Force due to the total weight of the vehicle on one wheel is,

$$F = \frac{mg}{4}$$

For equilibrium in y- direction,

$$F = F_s\cos(\theta_4 - 90 - \theta_0) = F_{sy}$$
$$\frac{mg}{2} = 0.5Kc\sin(\theta_4 - 90 - \theta_0)$$

Here the values of mass (m) and stiffness (K) are obtained from the previous subsystem's results.

Moment equilibrium,

$$F_s\left(\frac{c}{2}\right) = F(c\cos(\theta_4 - 90 - \theta_0) + w)$$
$$\frac{Kc^2\sin(\theta_4 - 90 - \theta_0)}{4} = \frac{mg}{4}(c\cos(\theta_4 - 90 - \theta_0) + w)$$
$$\boldsymbol{Kc^2\sin(\theta_4 - 9\ 0 - \theta_0) = mg(c\cos(\theta_4 - 9\ 0 - \theta_0) + w)}$$

The equations in bold letters are the constraints used in optimization problem.

2.2.3 Bounds

The bounds for the variables have been obtained from the dimensions of a general ATV (Auto Terrain Vehicle). The bounds are listed below,

$$0 \le a\ (mm) \le 5\ 00$$
$$0 \le b\ (mm) \le 300$$
$$0 \le c\ (mm) \le 35\ 0$$
$$0 \le d\ (mm) \le 300$$
$$9\ 0 \le \theta_2\ (°) \le 16\ 0$$
$$0 \le \theta_0(°) \le 45$$
$$9\ 0 \le \theta_4(°) \le 120$$
$$10 \le \theta_3(°) \le 30$$

2.3 Optimization Study

Now, the objective function was initially checked for Monotonicity with respect to the variables in MATLAB by plotting the function with respect to the variables one by one considering a fixed point in the domain of these variables. The following plots were obtained,

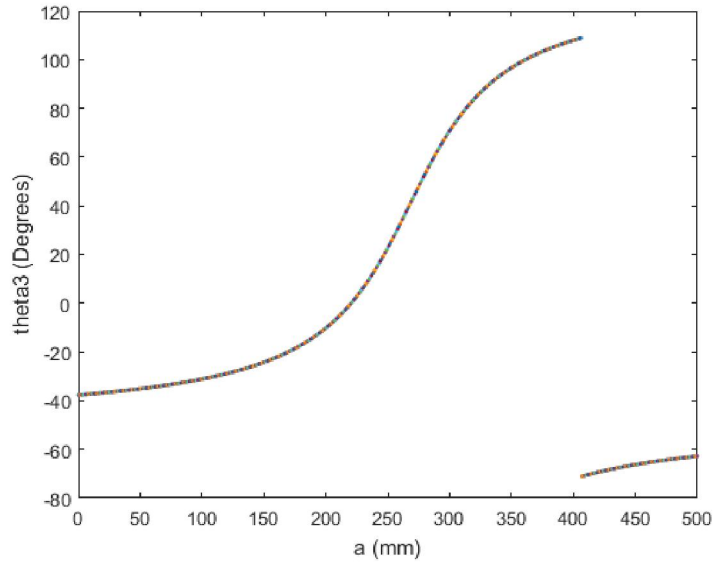Fig. 2.3 Plot of θ_3 versus a
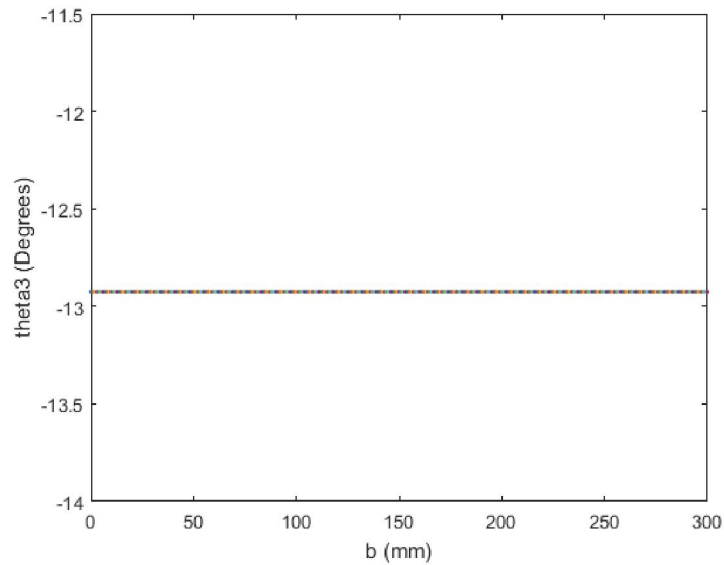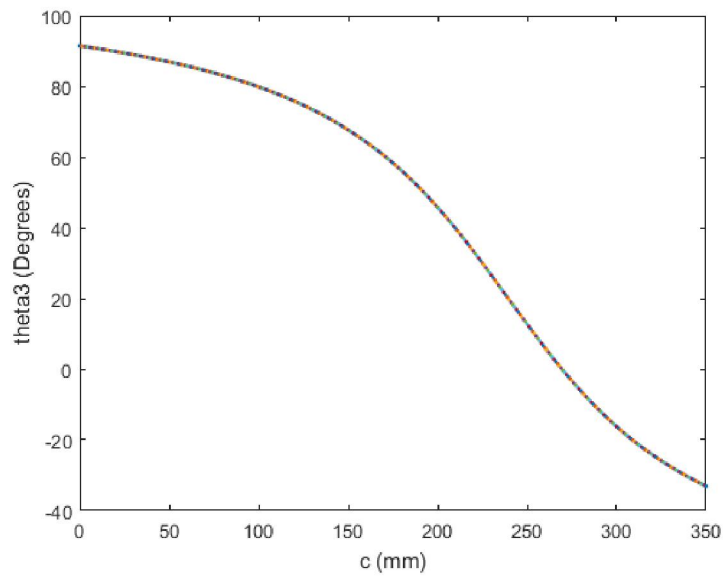

Fig. 2.4 Plot of θ_3 versus b

Fig. 2.5 Plot of θ_3 versus c
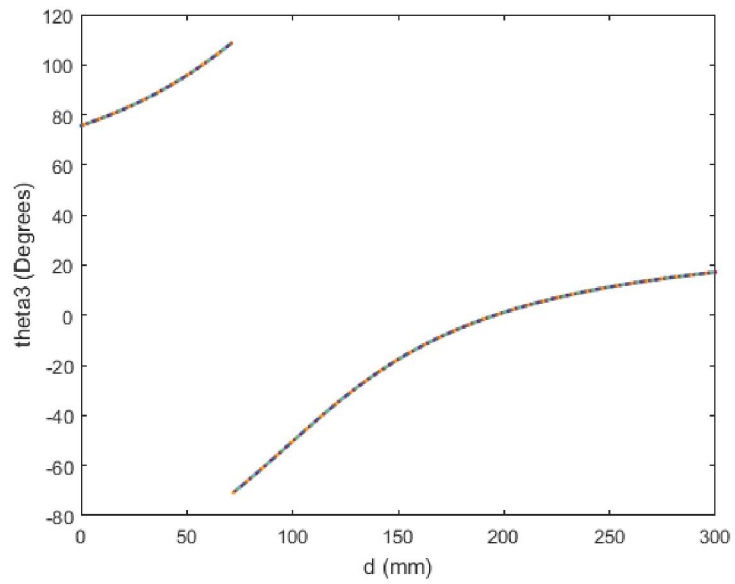
Fig. 2.6 Plot of θ_3 versus d

Fig. 2.7 Plot of θ_3 versus θ_2

Fig. 2.8 Plot of θ_3 versus θ_0

15
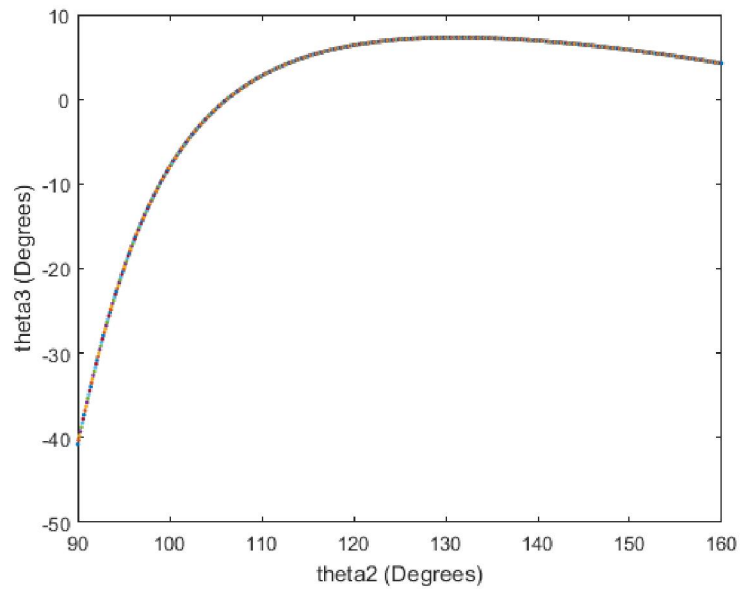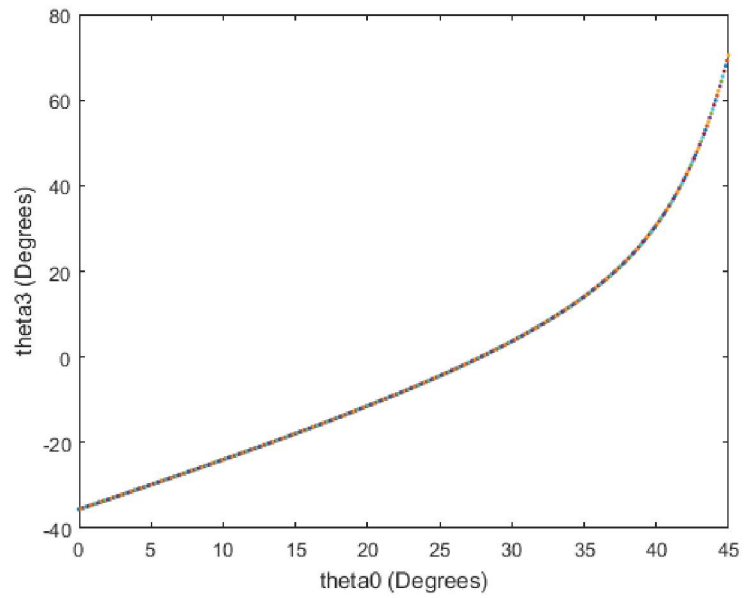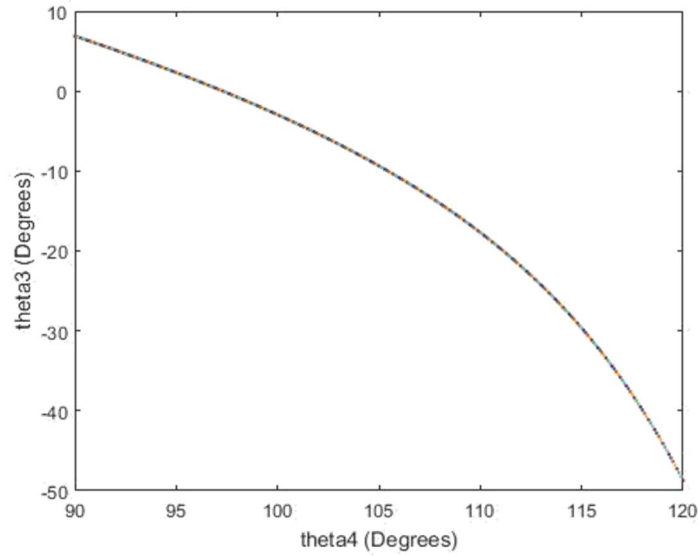
Fig. 2.9 Plot of θ_3 versus θ_4

As can be seen, the objective is non-monotonic with respect to some of the variables. So, a proper method for solving this optimization problem can be MATLAB's function *fmincon* with SQP algorithm.

2.4 Results and Discussion:

After solving by *fmincon*, the following results were obtained for different initial conditions,

Table no. 2.1 Optimized geometric parameters of suspension considering different initial points

Sr. no.	a	b	c	d	θ_2	θ_0	θ_4	$\theta_3(*)$
1	150	150	270	150	100	20	110	20.7916
2	150	150	270	150	100	20	115	22.8526
3	151	151	271	151	101	21	116	24.546
4	153	153	273	153	103	23	113	23.5319
5	156	156	276	156	106	26	116	26.5763
6	148	148	268	148	98	18	108	18.8900

It can be observed from the above table, that the minimum value for the objective function that is the variation in camber, obtained is 18.89°. So the values of the parameters obtained from this optimization are as follows,

16

Table no. 2.2 Optimum results of geometric parameters of Suspension

a	b	c	d	θ_2	θ_0	θ_4	$\theta_3(*)$
193	143.4	292.9	159.8	97.59	18.88	107.33	18.89

So, we can conclude from the above results obtained that the optimum variation in camber angle is 18.890 and this can be achieved by implementing the corresponding optimized geometric parameters as mentioned. This will increase the area of contact of tire with the road and eventually increase controllability and stability of the vehicle.

3. Subsystem 3 : Minimizing the Rolling Resistance of the tire (Aniket Borude)

3.1 Introduction

Rolling Resistance is the resistive force to the motion of a body rolling on a surface. The two main causes of rolling resistance are hysteresis losses and permanent plastic deformation. In the case of tires, there is no permanent plastic deformation but the hysteresis losses are prevalent. The hysteresis losses occur due to the constant loading and unloading over the body. Tires are such parts where the weight of the vehicle acts over the circumference of the rubber in a cycling manner. This causes hysteresis losses in the tire. The losses due to hysteresis also depend strongly on the material properties of the wheel or tire and the surface

Hysteresis losses are reduced by reducing the area between the loading and unloading curve in the stress strain diagram. This can be achieved by reducing the deformation in the tire when the tire is loaded. Hence, effectively the objective of this subsystem is to reduce the deformation in the tire when the tire is loaded.

3.2 Finite Element Model

The model of the tire was created in ANSYS Design Modeler. Since the tire is a part which is symmetric about an axis, the type of analysis that can be conducted on it can be of axisymmetric type. Sometimes there are parts in which the geometry and shape, the forces acting on the body and its constituent material are symmetric about a single axis. In these cases, the part can be solved as an axisymmetric problem. The advantage of this analysis is that the entire body of the tire need not be analyzed. A suitably short cross section can be chosen and the boundary and loading conditions can be applied to it to solve the problem.

The material chosen for the tire rubber is Styrene-Butadiene Rubber. Styrene-Butadiene[23] rubber is used in tires of off road vehicles. Natural rubber which is used on normal cars does not have the abrasion resistance capacity as styrene-butadiene rubber. The material properties of styrene-butadiene rubber are given in the table

Table 3.1 Material Properties of the rubber material

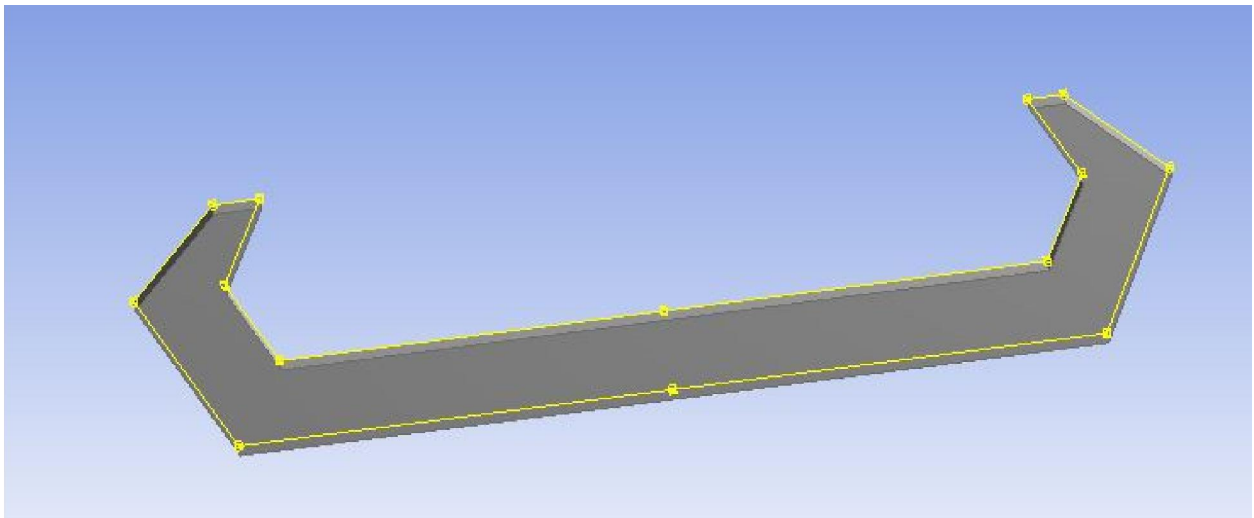| Material Property	Value
Density	950 kg/m^3
Shear Modulus	3.3 MPa
Poisson's Ratio	0.45
Young's Modulus	9.57 MPa
Bulk Modulus	31.9 MPa

Fig 2.1 Geometry of the tire cross section
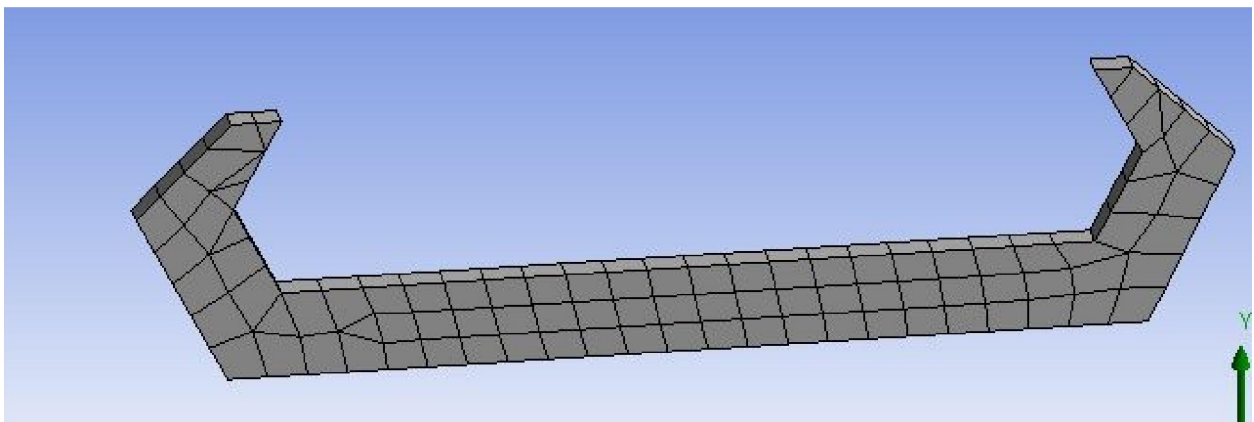
Fig 2.2 Meshed Geometry

3.3 Structural Analysis

ANSYS Static Structural Analysis was used to conduct the structural analysis on the part. The tire when loaded vertically due to the weight of the vehicle undergoes deformation in the vertical direction. Hence the major force acting on the tire geometry is the weight of the vehicle which is obtained from subsystem 1. Boundary conditions are applied to the lower part of the tire geometry cross section where a fixed support exists in the form of underformable surface of the road where the tire rests. The loads and the boundary conditions were applied to the tire geometry as shown in the figure.
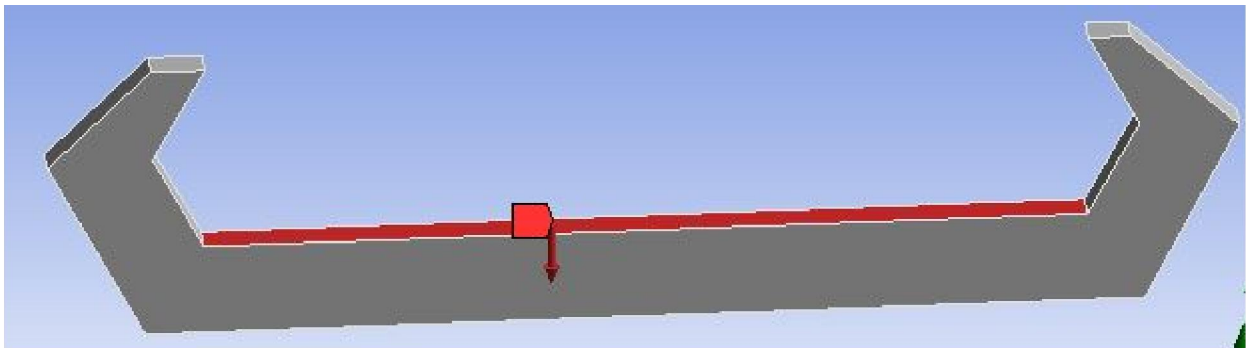
Fig 2.3 Force acting on the surface

Upon solving the structural analysis in ANSYS the deformation value is achieved. The geometry after deformation denotes that the deformation is primarily concentrated on the upper surface of the rubber material. This is the deformation that needs to be minimized to reduce the rolling resistance in the tire. The deformation in the tire is as shown in the Figure 2.4
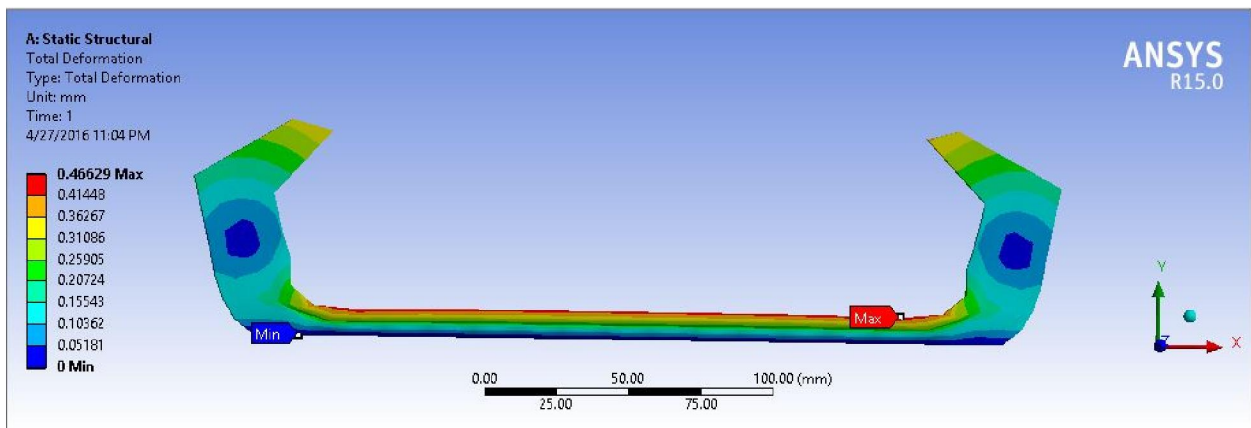
Fig 2.4 Deformed Tire Cross section

The Maximum stress value in the tire after loading (0.2195 MPa) is well below the yield and ultimate stress value for the rubber material. Hence the design is safe for work as well.
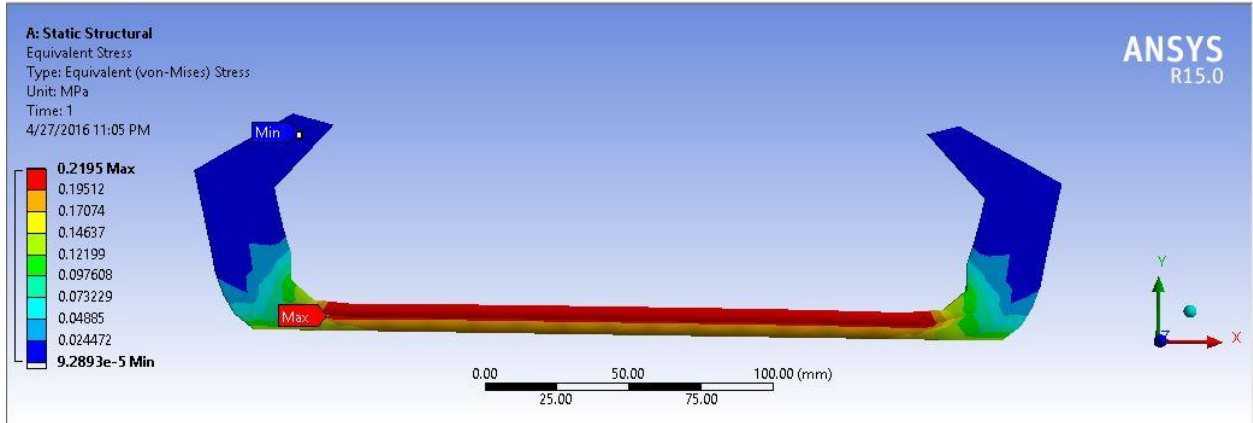
Fig 2.5 Stresses induced in the tire material

3.4 Design of Experiments

As a part of this project, a study has to be conducted how the output of the system, in this case the deformation of the tire is related to the input. The input in this case was the thickness of the rubber material and the shear modulus of the tire material. The thickness directly impacts the deformation in the tire because it is the parameter on which the load acts. Also, when the tire is in loading, the tire cross section is subjected to a shear force due to the weight of the tire. For this study the shear modulus of the tire is taken into account which denotes the shear strength of the material. The deformation in the tire depends on its shear strength which is dictated by the shear modulus

Hence, the two parameters which are taken into consideration are the thickness of the tire and the shear modulus of styrene-butadiene which is the material chosen for the tire.

The Design of Experiments type used was Latin Hypercube Sampling. Latin hypercube sampling (LHS) is a statistical method for generating a sample of plausible collections of parameter values from a multidimensional dimensions. In this case, the number of simulations required are independent from input parameters. The Design of Experiments was carried out for 50 points which is included in the Appendix C.

3.5 Response Surface

The Design Points and their solutions are obtained in the Design of Experiments step. Upon achieving the required results, a response surface is fitted across the results. Kriging model was used to create a response surface. The response surface provides a variation of the output parameters with respect to the changing input parameters. The response surface obtained is as shown in the Figure 2.6.

20
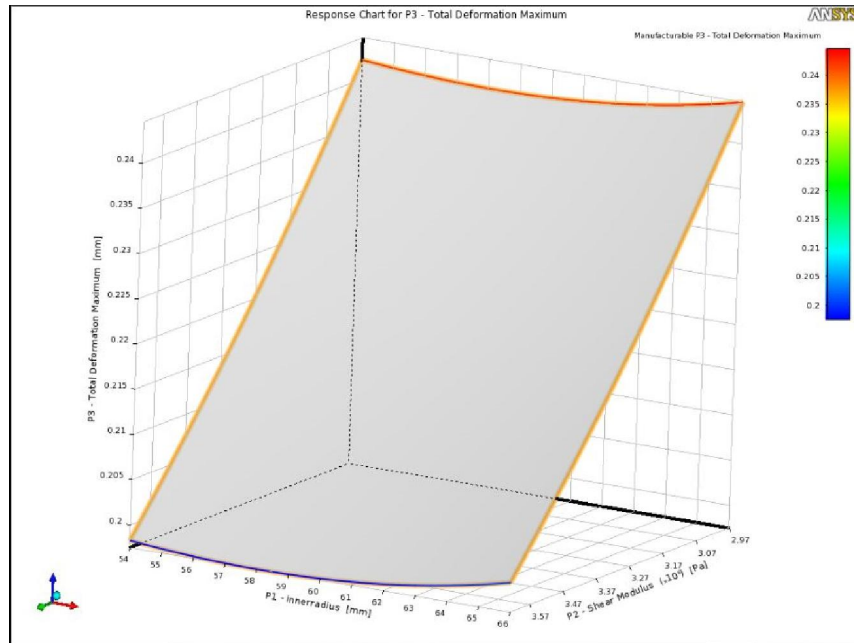
Fig 2.6 Response surface

The two parameters, thickness (inner radius in the figure) of the rubber and shear modulus of the tire are on the X and Z axes respectively. The output of Deformation in the tire is plotted along the Z axis. Further using this response surface, the optimization is carried out.

Figure 2.7 shows the goodness of fit plot. On the X axis the values of maximum deformation (red) and the maximum shear stress (blue) are plotted which are observed from the design points. Similarly along the Y axis the values of maximum deformation and maximum shear stress are plotted which are obtained from the response surface.

Fig 2.7 Goodness of fit

3.6 Optimization

Objective of the study is to minimize the total deformation in the tire. Hence the value of deformation from the structural analysis was entered as an output parameter. In ANSYS, the objective of the optimization study was assigned as to minimize the total deformation in the tire. The optimization algorithm used was MISQP (Mixed Integer Sequential Quadratic Programming).

Upon conducting the optimization study, a set of best candidate points were selected as shown in Figure 2.8

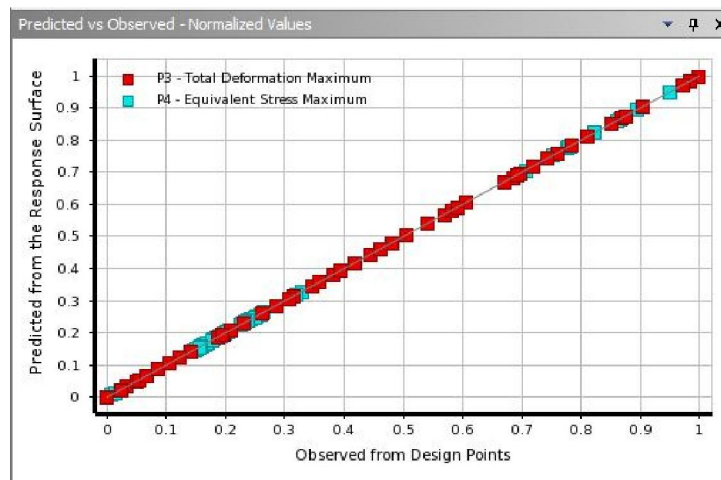| Reference	Name	P2 - Shear Modulus (Pa)	P1 - innerradius (mm)	P3 - Total Deformation Maximum (mm)		P4 - Equivalent Stress Maximum
				Parameter Value	Variation from Reference	
○	Candidate Point 1	3.63E+06	58.785	0.42396	0.00 %	0.21956
○	Candidate Point 1 (verified)			0.42401	0.01 %	0.21977
○	Candidate Point 2	3.63E+06	58.801	0.42396	0.00 %	0.21957
○	Candidate Point 2 (verified)			0.42408	0.03 %	0.22002
⦿	Candidate Point 3	3.63E+06	58.717	0.42396	0.00 %	0.21954
○	Candidate Point 3 (verified)			0.42402	0.01 %	0.21978

Fig 2.8 Candidate Points

3.7 Results

The Optimization study conducted using ANSYS yielded three candidate points. The candidate point number three was selected from the set of candidate points since this is the point which will require the least amount of material since the thickness is the least. The results obtained are verified and the variation of it from

4. Subsystem 4: Optimization of Strain Energy in the tire to improve the durability potential by varying the steel belt angles (Gaurav Kankriya)

4.1 Introduction

Tire is the only member in contact with both the vehicle and the road. Due to this fact, it has to meet many designing requirements of absorbing the road irregularities, Support the moving vehicle, reducing the shocks along with providing braking or steering control. So, the product life as well as mileage and environmental concerns majorly depend upon tire performance characteristics that are wear, durability and rolling resistance. Tire is made by reinforcing the series of plies of cords. This improves the strength and rigidity of the tire. This network that gives tire its shape is called the carcass. To improve further rigidity, steel belts are placed inside

the tire body. Radial plies are placed at right angles to the direction of motion. Due to this design, plies do not rub against each other as tire flexes, thus reducing the rolling resistance. But with only this arrangement, tire would not be sufficiently rigid at the contact with the ground. To provide further stiffness, additional belts oriented closer to the direction of travel are added. These belts are made up of steel and blended with the polyester. The orientation of these belts is an important design criteria. The figure 4.1 shows the cross-section view of the radial tire.
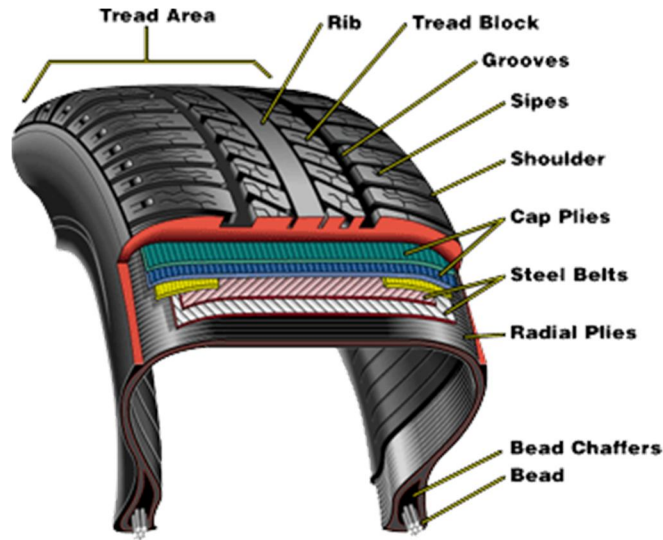
Figure 4.1 Cross Section of Radial Tire

While running, the tire is under continuous delta of loading and unloading cycle. The tire durability and the rolling resistance significantly depends upon the energy dissipated by the tire while running. The energy distribution around cross section of tire play vital role in tire durability. When tire comes in contact with the road, there is a deformation of tread block and thus tire components get strained and are relaxed while leaving the contact from road. This continuous cycle of loading and unloading introduces a delta of strain. This strain can be measured in terms of strain energy distribution. This generated strain energy has to be distributed and dissipated properly, otherwise it builds the heat inside the tire and eventually reduces the rubber mechanical properties. This makes tire more vulnerable to failure. Therefore, it is very important to consider this strain energy and optimize the same to have longer tire life. Tire being a very nonlinear in structure, it is very difficult to strike the balance between different parameters. So, optimizing the strain energy is very important. So, this study is focused on the steel belt angles and the variation of these belt angles to minimize the strain energy distribution around the tire cross section.

4.2 Optimization Procedure

The flow chart for performing the optimization operation on the given system is shown in figure 4.2
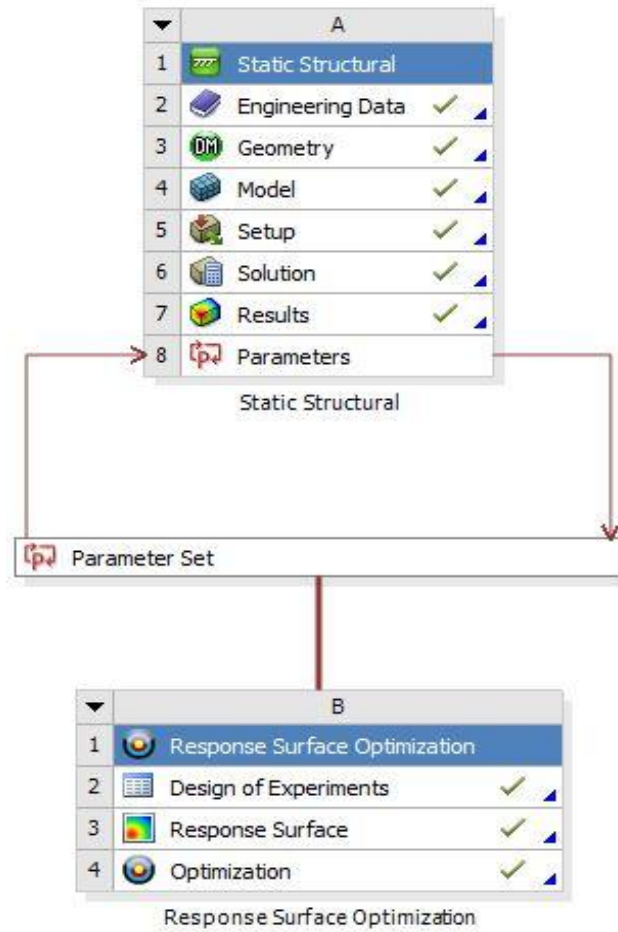
Figure 4.2 Optimization Procedure

4.3 Optimization Problem

The objective of this study is to optimize the strain energy distribution across the cross section of the tire by varying the steel belt angle1 and steel belt angle2. Here the angles are represent by the angles made by the plane containing the steel wire with the tire cross section planes.
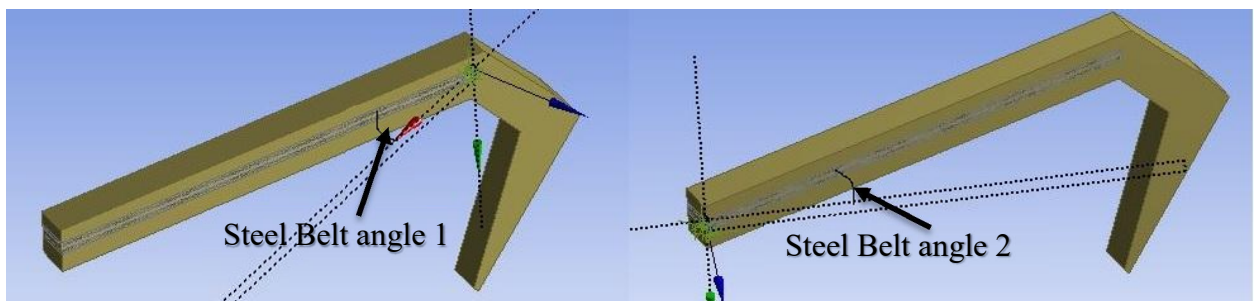
Figure 4.3 Steel Belt Angles

24

4.4 Finite Element Model

The tire is a very non-linear and complex part to design and examine. In order to simplify the problem, a 1/80 model of the actual tire model is designed. Taking advantage of tire symmetry, only half axisymmetric model is prepared. So, the 1/80 axisymmetric model is described in figure 4.4. The steel belts are rolled inside the tire rubber body. When the 1/80 model of tire is under consideration, the angle subtended at the center by the tire arc is 360/80 i.e. 4.5 degrees. So the tire arc can be approximated as a straight line and hence an approximated model of a tire is created as follow. Here, the angles subtended by steel wires with the cross section plane (Steel_belt_angle1 & Steel_belt_angle2) are considered as parameters.

Initially belt angles of 23 degrees and -23 degrees are provided in the model.
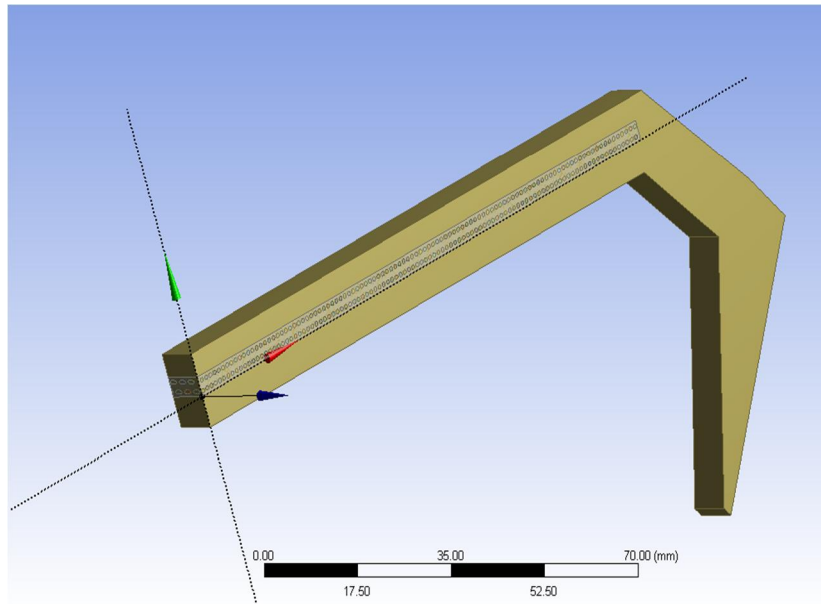
Figure 4.4 1/80 axisymmetric Tire Model
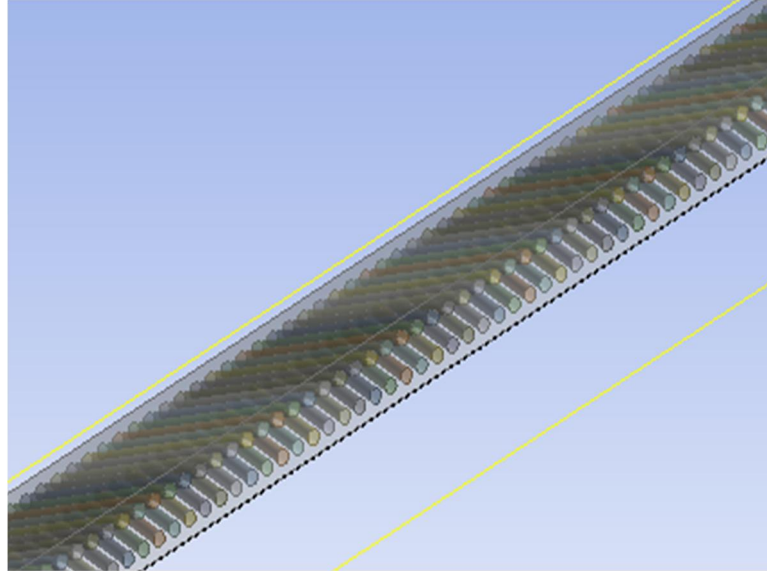
Figure 4.5 Steel Belt orientation

The detailed view of the steel wire orientations is described in figure 4.5. The CAD model is then meshed using tetrahedral quadratic elements. The computation time for mesh generation is very high therefore localized fine meshing is implemented and is shown in figure 4.6.
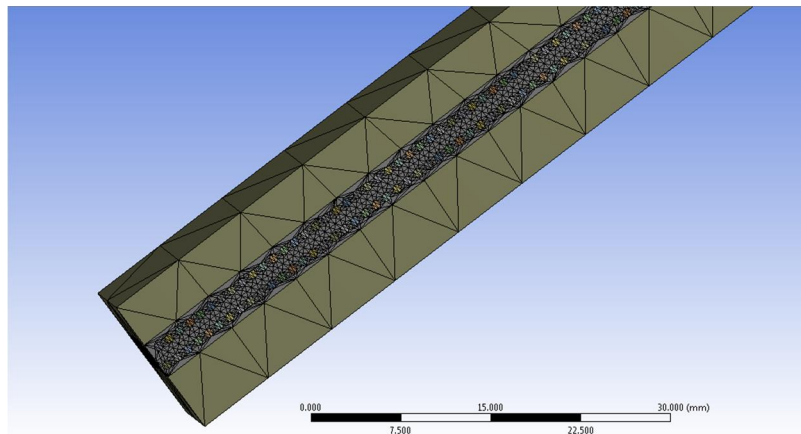
Figure 4.6 Localized mesh of Model

Material Properties:
There are basically three different bodies in the tire model. The outer tire body and the rubber material inside the steel wire are made up of styrene-butadiene rubber. The streel wires inside the steel belts are made up of High Carbon Steel. The important material properties can be summarize as follow:

Table 4.1 styrene-butadiene rubber properties

Material Property	Value
Density	950 kg/m^3
Shear Modulus	3.3 MPa
Poisson's Ratio	0.45
Young's Modulus	9.57 MPa
Bulk Modulus	31.9 MPa

Table 4.2 High Carbon Steel properties

Material Property	Value
Density	7850 kg/m^3
Shear Modulus	7692.3 MPa
Poisson's Ratio	0.3
Young's Modulus	200000 MPa
Bulk Modulus	166667 MPa

4.5 Structural Analysis

Generally the inflation pressure of an ATV tire is around 0.1-0.2 MPa. So an inflation pressure of 0.1 MPa is applied to the inner face of the tire. It is assumed that the vehicle weight is shared equally by the tires. So, the vehicle weight is taken from the first subsystem and from the data then an equivalent load of 428.75N was applied at the tire surface in contact with the road. The rim and the road surface are analytically modelled as rigid bodies. Also, the symmetric condition is applied at the mid plane of the tire as shown in figure 4.7.
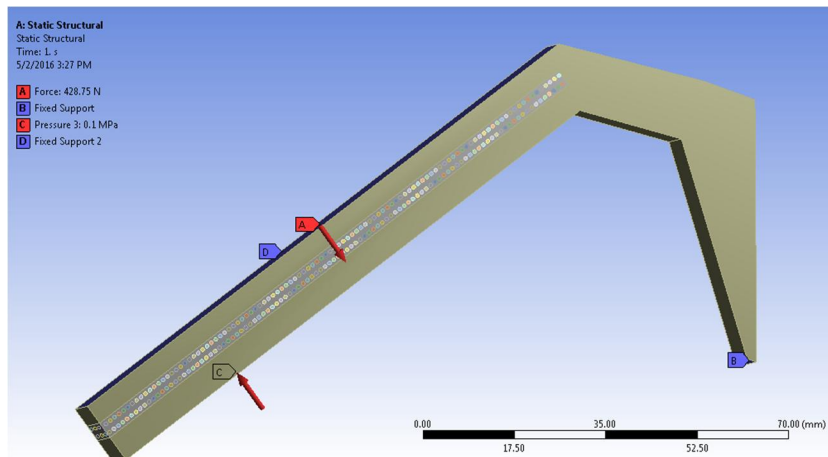
Figure 4.7 loading and Boundary conditions

After applying these loading and boundary conditions, the model is solved for the deflection in Y direction, and the strain energy distribution

4.6 Design of Experiments

After performing an initial analysis on the tire with the above set conditions, the relation between the design parameters and the response parameters is determined. For accurate relation between the input and output parameters, the same analysis has to be run with different initial design variables. So, this can be achieved with the help of Design of experiments. In this method, the analysis is run for different set of random input conditions and corresponding output parameters are recorded. For generating random set of points, Latin Hypercube Sampling (LHS) is implemented. User defined sample points are used to generate the response surface. Considering the complexity of the model and the computation time, the DOE is performed for 30 sampling points. The advantage of using the LHS over other sampling is that it spreads the sample points more evenly across all possible values. It also shuffles the sample for each input to avoid the correlation between inputs. Also, the number of simulations required are independent of number of input parameters. So, it is advantageous to use LHS over other DOE sampling methods. After performing the DOE, we get response parameters for different sampled initial conditions. The DOE points are listed in the Appendix D.

4.7 Response Surface

After performing the DOE, a response surface is generated using the Kriging model for all the DOE points. Kriging model helps to compensate for effect of data clustering also gives an estimate of the error estimation. The optimization is then performed on the response surface generated using he model. Goodness of fit is evaluated for the given response curve and is shown in the figure 4.8.
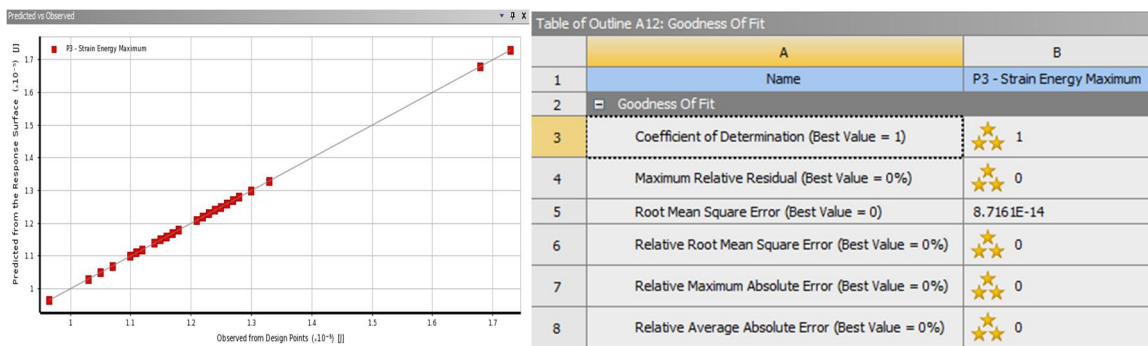
Figure 4.8 Goodness of fit

4.8 Structural Optimization

The response parameter of strain energy density is considered as an objective function which is to be minimized. A variation of optimal strain energy and other parameters is plotted using the MISQP (Mixed-Integer Sequential Quadratic Programming) algorithm. As seen in figure 4.9, it is quite evident from the sensitivity analysis that variation of both the parameters affect the response surface. The optimum candidate points are obtained using the MISQP algorithm in ANSYS. The best candidate point is chosen from the set of verified candidate points given by ANSYS optimization solver.
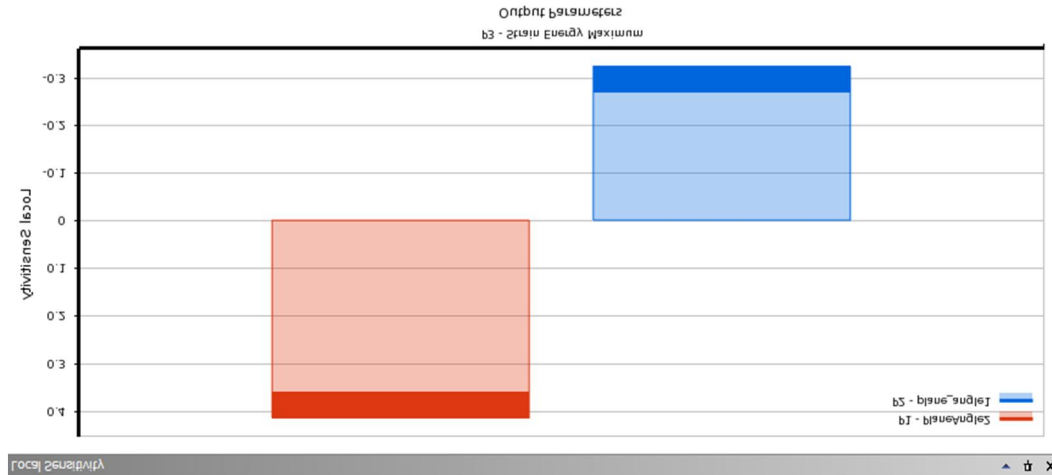
Figure 4.9 Sensitivity Analysis

4.9 Results

After performing the complete optimization procedure, the ANSYS results are summarized in the form of three different Candidate points. Candidate points are the best possible solutions found by the ANSYS solver and are listed in figure 4.10.So, it is now our decision to choose the best candidate point satisfying all our requirements. Result obtained well within the bounds given to parameters is considered as a good solution. Keeping this into mind, the candidate point 2 is selected as the optimum solution for the given minimization problem.

Table of Schematic B4: Optimization , Candidate Points

	A	B		C		D		E	F
1	Reference	Name	▼	P1 - PlaneAngle2 (degree)	▼	P2 - plane_angle1 (degree)	▼	P3 - Strain Energy Maximum (J) ▼	
2								Parameter Value	Variation from Reference
3	○	Candidate Point 1	DP 31	-25.166		20.811		7.0065E-06	-4.10 %
4	○	Candidate Point 2	DP 32	-22.192		24.242		7.019E-06	-3.93 %
5	◉	Candidate Point 3	DP 33	-22.195		24.209		7.3058E-06	0.00 %

Figure 4.10 Candidate Points

The optimization results can be summarized as follows:

Table 4.3 Optimization Results

Parameters	Initial Condition	Optimized Condition
Steel Belt Angle 1(degree)	23	24.242
Steel Belt Angle 2(degree)	23	-22.192
Strain Energy Distribution (mJ)	0.012	0.00730

The strain energy reduces significantly after optimizing the steel belt angles. This reduced strain energy distribution ensures the improved durability of the tire.

5.   System Integration

As we know that the suspension system under consideration is made up of the double wishbone suspension system and tire. So, when all the systems are optimized individually, the results must be integrated together for optimizing the suspension system performance.

The first subsystem deals with optimizing the vertical acceleration of the vehicle where with the sprung mass, unsprung mass and the spring stiffness being important parameters. Optimizing the vertical acceleration of the vehicle ensures better control. So, the optimal value of the sprung mass and spring stiffness are used as input parameters in the second subsystem and using these parameters along with other geometric parameters of the double wishbone system, the variation in the camber angle is optimized thus improving the controllability of the vehicle. As the tire is the only contacting element between the road and the vehicle, its performance optimization is very important. The total vehicle mass from the first subsystem is used as an input to the third and the fourth subsystem. The rolling resistance performance of the tire is optimized by optimizing the tire thickness and shear modulus of the rubber. The strain energy distribution is optimized in the fourth subsystem by effectively optimizing the steel belt angles of the tire improving the durability of the tire.

So, putting together all the subsystem optimization results, we can say that the comfort, controllability of vehicle and rolling resistance performance and the durability of the tire are optimized in this report, leading to the improved suspension system performance of an off-road vehicle.

6. References

1. M. MahmoodiKaleibar, I. Javanshir, K. Asadi, A. Afkar, A. Paykani, **"**Optimization of suspension system of offroad vehicle for vehicle performance improvement", Central South University Press and Springer Verlag Berlin Heidelberg 2013

2. . Michael McCarthy (July 13, 2009), "Four-Bar Linkage Analysis: The 4R Quadrilateral"

3. J. Michael McCarthy (July 13, 2009), "Four-Bar Linkage Analysis: The 4R Quadrilateral"

4. Anchang Liang, Shyhrong Yen (Dec 12 1987) "Suspenion Design of a 2-Dof Vehicle Model using jerk and acceleration"

5. Xiao-Pei, Heng-Lung Li, P. Papalambros (Jan 2 1984) "A design Procedure for the optimization of vehicle suspensions"

6. Djamel E.Midoun "Optimization of vehicle suspension using damped observer"

7. Zhongzhe Chi, Yuping He and Greg F. Naterer (December 2007) "Design optimization of vehicle suspensions with quarter car model"

8. Feng Tyan, Yu-Fen Hong, Shun-Hsu Tu and Wes S. Jeng "Generation of Road Profiles"

9. Mallikarjun Veeramurthy "Modelling, finite element analysis, and optimization of Non-Pneumatic Tire (NPT) for the minimization of rolling resistance"

10. P. Ghosh, A. Saha and R. Mukhopadhyay "Prediction of tyre rolling resistance using FEA"

11. Makwana B., P. Sankarganesh, Amarnarh S.K.P, Shah M., " optimization of Tyre Performance by varying Influence Parameter (Apllo Tyres)"

12. Pavel Koštial, Jan Krmela, Karel Frydrýšek and Ivan Ružiak, "The Chosen Aspects of Materials and Construction Influence on the Tire Safety"

13. Optimization in ANSYS Workbench

14. J.E. Mark, B. Erman, F.R.Eirich, "The science and technology of rubber"

15. Shida,Z., Koishi.M.,Kogure, T.,1999, "A Rolling Resistance Simulation of tires using Static Finite Element Analysis"

16. http://www.daerospace.com/MechanicalSystems/FourBarLinkageDesc.php

17. https://www.extremeiceland.is/en/activity-tours-iceland/atv-tours-iceland

18. http://facultad.bayamon.inter.edu/elay/mecn4110/ch04%20Position%20Analysis.pdf

19. http://www.speed-industries.ch/wordpress/wpcontent/uploads/2011/03/mcpherson_2wish.jpg

20. http://www.glanworthtyres.com/retail-customers/tyres/

21. https://en.wikipedia.org/wiki/Radial_tire

22. http://www.britannica.com/science/styrene-butadiene-rubber

23. https://en.wikipedia.org/wiki/Styrene-butadiene

7. Appendix

A. Subsystem 1
Matlab Code for Subsystem 1
Code for main function

```
A= [];
b= [];
x0= [98; 803; 204394; 63528; 3428];
Aeq= [];
beq= [];
lb= [78.4 642.4 163515.2 50822.4 2742.4];
ub= [117.6 963.6 245272.8 76233.6 4113.6];
options=optimoptions('fmincon','Display','iter','Algorithm','sqp');
[x, fval]= fmincon(@camber, x0, A, b, Aeq, beq, lb, ub, @const,options)
```

Code for Constraints

```
function [c, ceq] = const(x)
m1=x(1);
m2=x(2);
Kt=x(3);
K=x(4);
C=x(5);
V=40;
A=6.5*10^-6;
g=9.81;
B=40;

 c=[pi*A*V/(g^2)*m1/C*((Kt/(m1+m2)-K/m2)^2+K^2/(m1*m2)+C^2*Kt/(m2^2*m1)) -
0.27;...
    0.5*(sqrt((m2*g)))*(C^2*Kt/(K*(m1+m2))+K)^(-1/2)- 1;...
        (pi*A*V/(m2^2))*(C*Kt*Kt/m1+(Kt*K^2)/C) - B];
ceq= []
```

Code for objective Function

```
function sigmaz= camber(x)
m1=x(1);
m2=x(2);
Kt=x(3);
K=x(4);
C=x(5);
```

```
A=6.5*10^-6;
g=9.81;
V=40;
sigmaz=pi*A*V/(m2^2)*(Kt*C+(m1+m2)*(K ^2)/C);
```

B. Subsystem 2
1. **Code to check monotonicity:**

When a is considered as the variable

```
for a=0:1:500
% a= 193;
b= 143.4;
c= 292.9;
d= 159.8;
th2= 97.59;
th0= 18.88;
th4= 107.33;
Ax= a*cosd(th2-th0-90);
Ay= a*sind(th2-th0-90);
Nx= -d*sind(th0);
Ny= -d*cosd(th0);
Bx= c*cosd(-th4+th0+90)-d*sind(th0);
By= -(Ay+c*sind(-th4+th0+90)+d*cosd(th0));
theta3= th0+atand((Ax-Bx)/(Ay-By));
figure (1)
plot(a,theta3,'.')
hold on
end
xlabel('a (mm)')
ylabel('theta3 (Degrees)')
% end
```

When b is considered as the variable

```
for b=0:1:300
a= 193;
% b= 143.4;
c= 292.9;
d= 159.8;
th2= 97.59;
th0= 18.88;
th4= 107.33;
```

```
Ax= a*cosd(th2-th0-90);
Ay= a*sind(th2-th0-90);
Nx= -d*sind(th0);
Ny= -d*cosd(th0);
Bx= c*cosd(-th4+th0+90)-d*sind(th0);
By= -(Ay+c*sind(-th4+th0+90)+d*cosd(th0));
theta3= th0+atand((Ax-Bx)/(Ay-By));
figure (2)
plot(b,theta3,'.')
hold on
end
xlabel('b (mm)')
ylabel('theta3 (Degrees)')
```

When c is considered as the variable

```
for c=0:1:350
a= 193;
b= 143.4;
% c= 292.9;
d= 159.8;
th2= 97.59;
th0= 18.88;
th4= 107.33;
Ax= a*cosd(th2-th0-90);
Ay= a*sind(th2-th0-90);
Nx= -d*sind(th0);
Ny= -d*cosd(th0);
Bx= c*cosd(-th4+th0+90)-d*sind(th0);
By= -(Ay+c*sind(-th4+th0+90)+d*cosd(th0));
theta3= th0+atand((Ax-Bx)/(Ay-By));
figure (3)
plot(c,theta3,'.')
hold on
end
xlabel('c (mm)')
ylabel('theta3 (Degrees)')
```

When d is considered as the variable

```
for d=0:1:300
a= 193;
```

```
b= 143.4;
c= 292.9;
% d= 159.8;
th2= 97.59;
th0= 18.88;
th4= 107.33;
Ax= a*cosd(th2-th0-90);
Ay= a*sind(th2-th0-90);
Nx= -d*sind(th0);
Ny= -d*cosd(th0);
Bx= c*cosd(-th4+th0+90)-d*sind(th0);
By= -(Ay+c*sind(-th4+th0+90)+d*cosd(th0));
theta3= th0+atand((Ax-Bx)/(Ay-By));
figure (4)
plot(d,theta3,'.')
hold on
end
xlabel('d (mm)')
ylabel('theta3 (Degrees)')
```

When theta2 is considered as the variable

```
for th2=90:0.1:160
a= 193;
b= 143.4;
c= 292.9;
d= 159.8;
% th2= 97.59;
th0= 18.88;
th4= 107.33;
Ax= a*cosd(th2-th0-90);
Ay= a*sind(th2-th0-90);
Nx= -d*sind(th0);
Ny= -d*cosd(th0);
Bx= c*cosd(-th4+th0+90)-d*sind(th0);
By= -(Ay+c*sind(-th4+th0+90)+d*cosd(th0));
theta3= th0+atand((Ax-Bx)/(Ay-By));
figure (5)
plot(th2,theta3,'.')
hold on
end
xlabel('theta2 (Degrees)')
ylabel('theta3 (Degrees)')
```

When theta0 is considered as the variable

```
for th0=0:0.1:45
a= 193;
b= 143.4;
c= 292.9;
d= 159.8;
th2= 97.59;
% th0= 18.88;
th4= 107.33;
Ax= a*cosd(th2-th0-90);
Ay= a*sind(th2-th0-90);
Nx= -d*sind(th0);
Ny= -d*cosd(th0);
Bx= c*cosd(-th4+th0+90)-d*sind(th0);
By= -(Ay+c*sind(-th4+th0+90)+d*cosd(th0));
theta3= th0+atand((Ax-Bx)/(Ay-By));
figure (6)
plot(th0,theta3,'.')
hold on
end
xlabel('theta0 (Degrees)')
ylabel('theta3 (Degrees)')
```

When theta4 is considered as the variable

```
for th4=90:0.1:120
a= 193;
b= 143.4;
c= 292.9;
d= 159.8;
th2= 97.59;
th0= 18.88;
% th4= 107.33;
Ax= a*cosd(th2-th0-90);
Ay= a*sind(th2-th0-90);
Nx= -d*sind(th0);
Ny= -d*cosd(th0);
Bx= c*cosd(-th4+th0+90)-d*sind(th0);
By= -(Ay+c*sind(-th4+th0+90)+d*cosd(th0));
theta3= th0+atand((Ax-Bx)/(Ay-By));
figure (8)
plot(th4,theta3,'.')
```

```
hold on
end
xlabel('theta4 (Degrees)')
ylabel('theta3 (Degrees)')
```

Code for fmincon

```
A= [1 0 -1 0 0 0 0 0; 1 -1 -1 1 0 0 0 0];
b= [0;0];
x0= [0.148; 0.148; 0.268; 0.148; 98; 18; 108; 18];
Aeq= [];
beq= [];
ub= [0.5 0.3 0.35 0.3 160 45 120 30];
lb= [0 0 0 0 90 0 90 10];
options = optimoptions('fmincon','Display','iter','Algorithm','sqp','TolCon',1e-1);
[x, fval,exitflag]= fmincon(@camber, x0, A, b, Aeq, beq, lb, ub, @const, options)
```

Objective Function

```
function theta3= camber(x)
Ax= x(1)*cosd(x(5)-x(6)-90);
Ay= x(1)*sind(x(5)-x(6)-90);
Nx= -x(4)*sind(x(6));
Ny= -x(4)*cosd(x(6));
Bx= x(3)*cosd(-x(7)+x(6)+90)-x(4)*sind(x(6));
By= -(Ay+x(3)*sind(-x(7)+x(6)+90)+x(4)*cosd(x(6)));
th = [18,111];
fun = @(th)equation(th,x);
theta = fsolve(fun,th);
theta4= theta(2);
Bx= x(3)*cosd(theta4-x(6)-90)-x(4)*sind(x(6));
By= x(3)*sind(theta4-x(6)-90)-x(4)*cosd(x(6));
theta3= x(6)+90+atand((Ax-Bx)/(Ay-By));
```

Code to solve the simultaneous equations

```
function F= equation(th,x)
Ax= x(1)*cosd(x(5)-x(6)-90);
Ay= x(1)*sind(x(5)-x(6)-90);
Nx= -x(4)*sind(x(6));
```

```
Ny= -x(4)*cosd(x(6));
Bx= x(3)*cosd(-x(7)+x(6)+90)-x(4)*sind(x(6));
By= -(Ay+x(3)*sind(-x(7)+x(6)+90)+x(4)*cosd(x(6)));
F(1)= th(1)-90-x(6)-atand((Ax-Bx)/(Ay-By));
F(2)= -x(4)*cosd(x(6))+x(2)*cosd(x(6)-th(1))-x(3)*sind(90-th(2)+x(6))+x(1)*sind(x(5)-90-
x(6));
```

Constraints

```
function [c, ceq] = const(x)
w= 230/2;
k= 76230;
g= 9.81;
m= 890;
c= [-m*g/2+k*x(3)*sind(x(7)-90-x(6));...
k*x(3)^2*sind(x(7)-90-x(6))-m*g*(x(3)*cosd(x(7)-90-x(6))+w)];
ceq= [x(1)*cosd(x(5))+x(2)*cosd(x(8))-x(3)*cosd(x(7))-x(4);...
    x(1)*sind(x(5))+x(2)*sind(x(8))-x(3)*sind(x(7))];
```

C. DOE points using LHS for subsystem 3

#	P2 - Shear Modulus (Pa)	P1 - innerradius (mm)	P3 - Total Deformation Maximum (mm)	P4 - Equivalent Stress Maximum (MPa)		
Name	P2	P1	P3	P4		
1	3214200	54.84	0.479637	0.22046		
2	3333000	61.8	0.462084	0.219699		
3	2989800	64.2	0.519608	0.22533		
4	3267000	61.08	0.471254	0.219609		
5	3016200	56.76	0.510743	0.220362		
6	3583800	57.72	0.42971	0.220238		
7	32538	62.76	0.473567	0.219871		

	00					
8	3570600	61.32	0.431232	0.219626		
9	3095400	58.44	0.497297	0.219838		
10	3055800	65.88	0.507519	0.225296		
11	3148200	54.12	0.490377	0.218116		
12	3042600	59.88	0.505777	0.219653		
13	3201000	59.4	0.48082	0.219905		
14	3372600	65.16	0.463392	0.225072		
15	3135000	56.28	0.491466	0.220363		
16	3491400	63.48	0.444824	0.225317		
17	3465000	60.12	0.44411	0.219474		
18	3319800	65.4	0.468027	0.226889		
19	3029400	58.92	0.508142	0.220033		
20	3003000	65.64	0.518187	0.226111		
21	3187800	61.56	0.483079	0.219682		
22	3504600	56.04	0.439652	0.22021		
23	3597000	64.44	0.431562	0.224646		
24	3069000	55.56	0.502185	0.220537		
25	3412200	60.36	0.451037	0.219493		
26	3306600	58.68	0.465494	0.219789		
27	3451800	58.2	0.445998	0.219881		
28	3359400	55.8	0.458732	0.220507		
29	3610200	57.96	0.426466	0.219921		

#	P1	P2	P3	P4			
30	3161400	63.24	0.489106	0.221157			
31	3425400	63.96	0.455848	0.225723			
32	3478200	63	0.444589	0.221069			
33	3227400	59.16	0.476926	0.219952			
34	3517800	62.52	0.437974	0.219838			
35	3174600	63.72	0.490985	0.226369			
36	3108600	55.08	0.49588	0.220427			
37	3557400	60.6	0.432679	0.21951			
38	3544200	57	0.434617	0.220326			
39	3293400	54.36	0.468007	0.218197			
40	3623400	64.92	0.42868	0.227338			
41	3280200	57.24	0.469524	0.219996			
42	3240600	64.68	0.481659	0.226061			
43	3385800	55.32	0.45524	0.220567			
44	3082200	57.48	0.499641	0.219951			
45	3438600	56.52	0.448068	0.220274			
46	3399000	62.04	0.453172	0.219754			
47	3531000	54.6	0.436465	0.218263			
48	3346200	59.64	0.459833	0.219582			
49	3121800	62.28	0.493584	0.220012			
50	2976600	60.84	0.517168	0.219571			

D. DOE points using LHS for subsystem 4

#	P1	-	P2	-	P3 - Strain Energy Maximum

	PlaneAngle2 (degree)	plane_angle1 (degree)	(J)		
Name	P1	P2	P3		
1	-22.7571	21.38571	1.28E-05		
2	-22.2429	23.52857	1.16E-05		
3	-23.9571	23.35714	1.18E-05		
4	-22.5	22.15714	1.26E-05		
5	-23.7857	23.95714	1.24E-05		
6	-21.2143	22.07143	1.12E-05		
7	-22.5857	21.72857	1.68E-05		
8	-21.3	22.58571	1.33E-05		
9	-23.3571	21.3	1.30E-05		
10	-23.5286	23.01429	1.25E-05		
11	-23.1857	22.67143	1.16E-05		
12	-23.6143	23.18571	1.15E-05		
13	-22.8429	22.5	1.73E-05		
14	-22.0714	21.47143	1.05E-05		
15	-23.2714	21.04286	1.27E-05		
16	-21.5571	21.21429	1.23E-05		
17	-21.7286	22.92857	1.17E-05		
18	-23.7	22.75714	1.03E-05		
19	-23.8714	21.64286	1.16E-05		
20	-22.9286	21.9	1.21E-05		
21	-21.4714	23.1	1.11E-05		
22	-21.1286	22.84286	1.14E-05		
23	-23.4429	21.81429	1.05E-05		
24	-21.9857	23.87143	1.10E-05		
25	-21.0429	23.61429	1.15E-05		
26	-23.1	21.55714	1.12E-05		
27	-21.9	23.44286	1.22E-05		
28	-22.6714	23.7	1.15E-05		
29	-21.3857	21.98571	9.65E-06		
30	-23.0143	23.78571	1.07E-05		